*36th EPS Conference on Plasma Phys. Sofia, June 29 - July 3, 2009 ECA Vol.**33E**, P-2.199 (2009)*

Multi-mode modeling of toroidal momentum confinement in tokamaks

F.D. Halpern[1], A.H. Kritz[2], G. Bateman[2], R.V. Budny[3], J. Weiland[4]

[1] *Centre de Physique Théorique, CNRS, École Polytechnique, 91120 Palaiseau, France*

[2] *Lehigh University Physics Department, 16 Memorial Drive East, Bethlehem, PA 18015*

[3] *PPPL, Princeton University, PO Box 451, Princeton, NJ 08543*

[4] *Chalmers University of Technology, Association EURATOM-VR, Göteborg, Sweden*

It is important to predict the plasma toroidal rotation in tokamaks because of the large impact of rotation on plasma confinement, fusion power production, and large scale instabilities such as resistive wall modes and neoclassical tearing modes. In tokamak discharges driven with a sufficiently large neutral beam torque, the gradient in toroidal plasma rotation produces a dominant contribution to flow shear, which reduces turbulent transport and increases confinement [1]. It is believed that most of flux of momentum observed in tokamaks [2] is driven by ion temperature gradient (ITG) or trapped electron modes (TEM).

In the present work, integrated modeling simulations of 16 DIII-D tokamak neutral beam heated discharges were carried out in order to study the toroidal angular momentum as a function of injected torque. The simulations were carried out using the PTRANSP integrated modeling code [3], in which many physical effects observed in tokamak experiments can be included simultaneously. In these simulations, thermal transport, from the magnetic axis to the top of the H-mode pedestal, is governed by the MMM08 combination of neoclassical, paleoclassical, and anomalous transport models described in Ref. [4].

Of particular interest for the present paper is the flux of toroidal angular momentum transport driven by ITG/TEM modes. The momentum diffusion and convection included in the simulations are derived by considering symmetry breaking effects due to toroidicity [5]. Note that the diffusion and convection terms obtained in Ref. [5] are equivalent to the turbulent equipartition and Coriolis pinch effects derived using the gyrokinetic formulation in Refs. [6, 7].

Plasma profiles for DIII-D discharge 125236 at 2.9 seconds are shown in Fig. 1 as an illustration of the comparison between simulation results and experimental data. Simulation profiles predicted by the PTRANSP code using the MMM08 transport model are represented by solid lines while experimental data profiles are represented by open circles. The predicted profiles represent one time slice taken from a time-dependent simulation that starts during Ohmic heating and continues through the L-mode and H-mode phases of the discharge. Note, in Ref. [8], the plasma profiles obtained in all simulations of the DIII-D discharges presented in this paper are compared with experimental data.

The DIII-D discharge 125236 shown in Fig. 1 is part of a series of experiments that are described in Ref. [9]. In these experiments, the neutral beam injection (NBI) torque was varied in steps during each discharge by turning the co-injected and counter-injected (relative to the toroidal plasma current) neutral beam sources on and off, in order to measure the change in plasma angular momentum as the torque is varied while maintaining the plasma β, density and current constant. The magnetic q profile in these discharges was kept above unity in order to suppress sawtooth oscillations. Altogether, nine data points are obtained from different time slices during the four discharges 125229, 125233, 125236, and 125238 in this experiment.

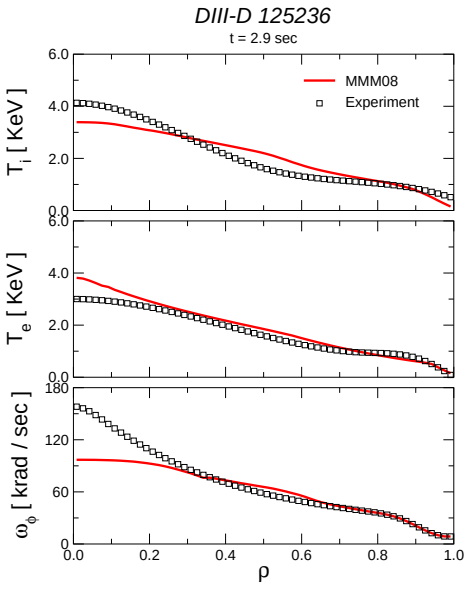

Figure 1: T_i, T_e, and ω_ϕ profiles for DIII-D discharge 125236 at $t = 2.9$ seconds.

Zero torque is obtained during the late stage of discharge 125233 within the inner 80% of the minor radius. In Fig. 2, the toroidal angular momentum L is plotted as a function of the injected torque found in predictive simulations using the MMM08 model (triangles) and corresponding TRANSP analysis (circles). The torque and the angular momentum are computed by integrating the torque and angular momentum densities from the magnetic axis to normalized minor radius $\rho = 0.8$, since that is the domain in which the angular frequency is predicted in the simulations. Least square linear fits for the data points are shown in the plot as a solid line for predictive simulations using the MMM08 transport model and as a dashed line for the TRANSP analysis.

The MMM08 predictive simulations reproduce the experimentally observed variation of toroidal angular momentum as a function of the injected torque as well as the negative torque needed to produce zero angular momentum. Simulations using the MMM08 model can produce the observed finite residual angular momentum at zero and the finite torque that must be applied against the direction of the plasma current in order to stop plasma rotation ($L = 0$) because turbulence drives momentum convection from the boundary region inward towards the plasma center. As an example, the

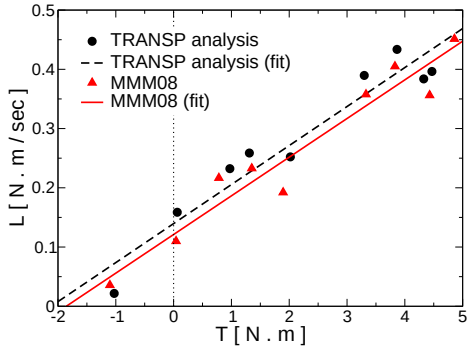

Figure 2: Toroidal angular momentum as a function of input torque for DIII-D discharges 125229-125236.

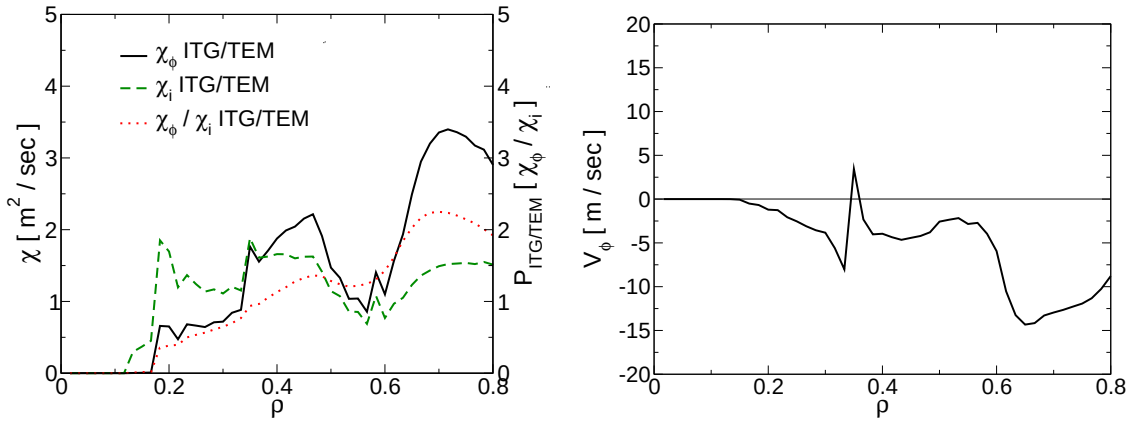

Figure 3: χ_i, χ_ϕ, χ_ϕ/χ_i (left panel), and toroidal momentum convective velocity (right panel) obtained in predictive simulation of DIII-D discharge 125236 at $t = 2.9$ seconds.

toroidal momentum diffusivity and the toroidal momentum convection are plotted in Fig. 3. The direction of the momentum convection in the MMM08 model is independent of the beam momentum sources if the convection term driven by the velocity gradient is neglected. (That term is small in cases with zero and negative torque).

The dependence of the momentum confinement time as a function of the injected torque is shown in Fig. 4 for the 16 tokamak discharges considered. In this plot, the momentum confinement time, τ_ϕ, is normalized by the plasma current I_ϕ, while the injected torque is normalized by the volume integral of the ion density, N. The vertical axis is shown using logarithmic scale in order to magnify detail. Results obtained from predictive simulations using the MMM08 transport model are shown as triangles, while results obtained from TRANSP analysis are shown as filled circles. One discharge has finite angular momentum with a torque very close to zero (but not exactly zero). The MMM08 and experimental data results follow similar trends, which can be fit with the following power law scalings:

$$\left(\frac{\tau_\phi}{I_\phi}\right)_{\text{MMM08}} = 0.068\left(\frac{\text{Torque}}{N/10^{20}}\right)^{-0.78} \quad (1)$$

$$\left(\frac{\tau_\phi}{I_\phi}\right)_{\text{Experiment}} = 0.072\left(\frac{\text{Torque}}{N/10^{20}}\right)^{-0.69}, \quad (2)$$

where τ_ϕ is the momentum confinement time in seconds, I_ϕ is the toroidal plasma current in MA, the torque is given in Newton meters, and N is the total number of thermal ions out to a normalized minor radius $\rho = 0.8$.

In conclusion, the transport of toroidal momentum and thermal transport in tokamak discharges is studied in predictive simulations. The model is validated by comparing PTRANSP integrated modeling simulation results with experimental data from 16 DIII-D neutral beam

heated discharges. The angular momentum profiles are evolved by balancing the NBI torque against momentum diffusion and convection driven by ITG/TEM modes.

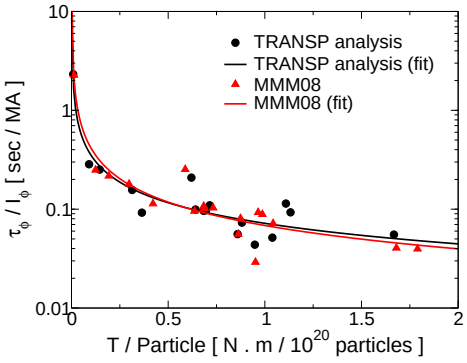

Figure 4: Toroidal angular momentum confinement time τ_ϕ as a function of torque per ion.

The fluid model used to compute the momentum fluxes incorporates symmetry breaking due to curvature and flow shear, which yields a strong diffusive flux and a convective flux, which can be inward or outward depending on the frequency of the drift wave eigenmode. The fluxes are equivalent to the turbulent equipartition and Coriolis pinch effects described in Refs. [6, 7]. The momentum pinch is normally inward for NBI heated H-mode plasmas with flat density profiles. This inward convection can drive peaked rotation profiles, even when there is no net torque input. Results of angular momentum modeling carried out using the MMM08 model reproduce the experimentally observed trends in the variation of angular momentum with applied torque, and the variation of the momentum confinement time as a function of the torque per ion.

References

[1] K. Burrell, Physics of Plasmas **4**, 1499 (1997).

[2] J. deGrassie, J. Rice, K. Burrell, *et al.*, Physics of Plasmas **14**(5), 056115 (2007).

[3] R. Budny, R. Andre, G. Bateman, *et al.*, Nuclear Fusion **48**(7), 075005 (2008).

[4] F. Halpern, *Integrated model for transport and large scale instabilities in tokamak plasmas*, Ph.D. thesis, Lehigh University (November 2008).

[5] J. Weiland, R. Singh, H. Nordman, *et al.*, Nuclear Fusion **49**(6), 065033 (2009).

[6] T. Hahm, P. Diamond, O. Gurcan, and G. Rewoldt, Physics of Plasmas **15**(5), 055902 (2008).

[7] A. Peeters, C. Angioni, and D. Strintzi, Physical Review Letters **98**(26), 265003 (2007).

[8] A. Kritz, G. Bateman, F. Halpern, *et al.*, in *Proceedings of the 36th European Physical Society Conference on Plasma Physics* (European Physical Society, Sofia, 2009), p. P2.200.

[9] W. Solomon, K. Burrell, J. deGrassie, *et al.*, Plasma Physics and Controlled Fusion **49**(12B), B313 (2007).